



3D bioprinting for modelling vasculature

Pranabesh Sasmal¹, Pallab Datta¹, Yang Wu^{2,3}, Ibrahim T. Ozbolat^{2,3,4,5}

¹Centre for Healthcare Science and Technology, Indian Institute of Engineering Science and Technology Shibpur, Howrah, India; ²Engineering Science and Mechanics Department, ³The Huck Institutes of the Life Sciences, ⁴Biomedical Engineering Department, ⁵Materials Research Institute, Penn State University, University Park, PA, USA

Contributions: (I) Conception and design: IT Ozbolat; (II) Administrative support: None; (III) Provision of study material or patients: All authors; (IV) Collection and assembly of data: All authors; (V) Data analysis and interpretation: All authors; (VI) Manuscript writing: All authors; (VII) Final approval of manuscript: All authors.

Correspondence to: Ibrahim T. Ozbolat. Penn State University, University Park, PA, USA. Email: ito1@psu.edu.

Abstract: Though *in vivo* models provide the most physiologically-relevant environment for studying tissue development and function, an *in vitro* substitute is being offered by the advancement of three-dimensional (3D) bioprinting technology, which is a reproducible and scalable fabrication strategy providing precise 3D control compared to conventional microfluidic tissue fabrication methods. In this review, vasculature models printed using extrusion-, droplet-, and laser-based bioprinting techniques are summarized and compared. Besides bioprinting of hydrogels as bioinks, an alternative method to obtain vascular models by bioprinting is to use exogenous biomaterial-free cell aggregates such as tissue spheroids and cell pellet, which has also been discussed here. In addition, there have been efforts to fabricate micro-vasculature constructs (e.g., capillaries) to overcome the practical limitations of bioprinting of large scale vascular networks. At the end of the review, limitations and prospective of bioprinting in vasculature modelling has also been expounded.

Keywords: Bioprinting; 3D printing; vasculature; bioink; tissue models

Received: 12 May 2018; Accepted: 11 October 2018; Published: 05 November 2018.

doi: 10.21037/mps.2018.10.02

View this article at: <http://dx.doi.org/10.21037/mps.2018.10.02>

Vascularization

The vascular system, being responsible for connecting all other tissues of the body, is indispensable to human life. Malfunction of vascular system is associated with tissue over-growth (e.g., angiogenesis in cancer) as well as cell death and necrosis. Role of vascular abnormalities have been identified in cardiovascular, neurovascular and musculoskeletal diseases, which happen frequently as age increases (1,2). The importance of vascular system thus spurs intensive interests in studying the molecular and genetic nature of blood vessels, and their pathological implications, in which two-dimensional (2D) culture models *in vitro* and animal models *in vivo* are used traditionally. However, neither the animal nor 2D models have been able to fully recapitulate all the features of human vasculature, which drives efforts of researchers towards generating three-dimensional (3D) models of the vasculature (3,4).

Therefore, there has been an interest in fabrication of functional vascular networks integrated within other organ models while successful fabrication of vessel like structures is expected to have applications in several domains as represented in *Figure 1*.

Recently, notable developments made in areas of microfluidics and 3D bioprinting offer unprecedented opportunities to fabricate functional 3D vascular constructs (6). Microfluidics and lab-on-a-chip devices allow flow to be controlled to match the physiological condition and provide spatiotemporal variations over chemical cues. Therefore, microfluidic devices are applied increasingly in building pathological models and drug screening. On the other hand, 3D bioprinting is a promising technique to fabricate 3D structures with various combinations of cells and materials under physiologically amenable conditions, which has also drawn intensive attention in tissue engineering and drug development. By integrating microfluidic devices and

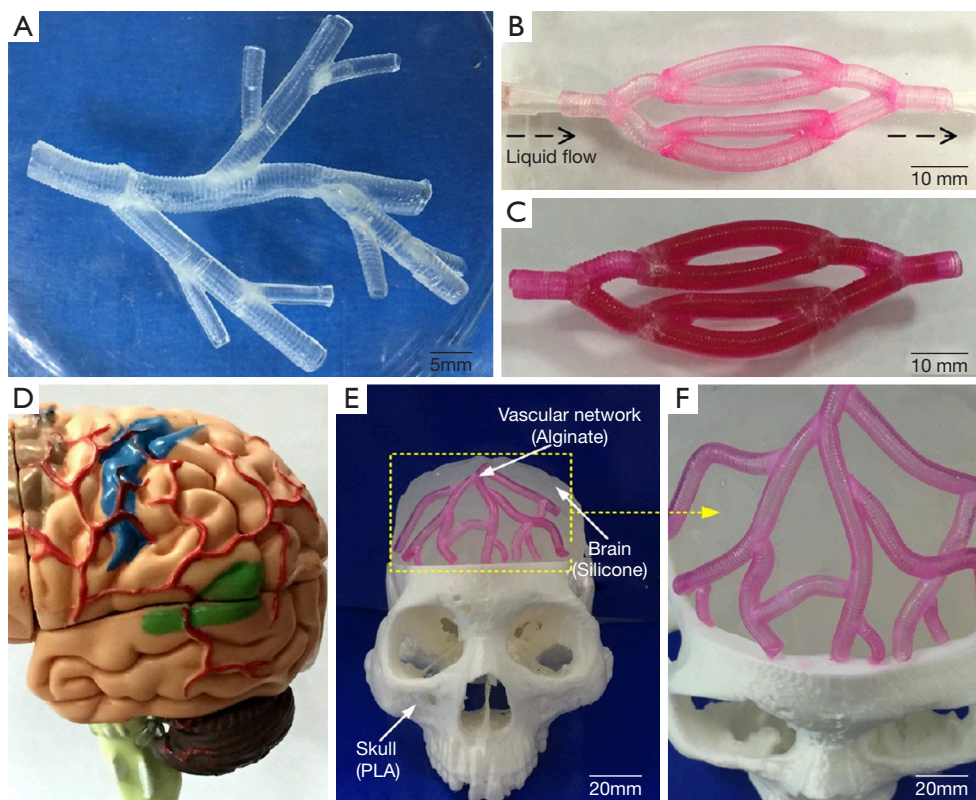


Figure 1 Successful fabrication of blood vessel-like structures is expected to have applications in several domains like (A) engineered vascular networks, (B) circulatory system, (C) perfusable *in vitro* culture systems, and (D,E,F) surgical simulation for cerebral [reprinted (adapted) with permission from Gao *et al.* (5)].

bioprinting, bioprinting is capable of fabricating complex devices to tune the flow conditions of microfluidics, in which microfluidic channels are able to imitate native vasculature. Moreover, for fabricating vascularized tissue models, in which vasculature is branching, free-standing microfluidic channels are not sufficient, and it needs the aid of bioprinting to fabricate mimetic constructs (7).

Anatomy of vasculature

In human body, the vasculature develops from an embryonic vascular plexus into a hierarchically complex structure as shown in *Figure 2*. Blood vessel consists of different concentric layers varying with respect to cellular and extracellular matrix (ECM) (8). The number of layers also depends upon the location of the blood vessel and physiological functions they perform. Intima is the innermost layer of the blood vessel composed of a single layer of endothelial cells which communicates with the lumen wall and provides the barrier between tissue and blood compartment. The

endothelial layer also prevents bacterial infestation and is lined by tight junctions to avoid exposure to sub-intimal layer, which may trigger thrombus formation. The intima is the basement membrane comprised of collagen type IV, laminin and fibronectin. A predominant elastin layer encircles the basement membrane. The next cellular layer is the tunica media consisting of smooth muscle cells (SMCs), possessing capacity of synchronized contractions along with elastin, proteoglycan and collagen type I and III (9,10). The collagen and SMC are helically oriented along the vessel axis. Tunica media layer is relatively thick in large arteries like aorta. Tunica adventitia is the outermost layer circumventing the tunica media, which consists of fibroblasts as the cellular component embedded in a loosely arranged matrix of collagen. The thickness of individual layer depends upon the location of blood vessel. For example, in capillaries embedded in tissues, whose principal function is rapid nutrient diffusion, only the endothelial intima layer composed of endothelial cells is present and provides a semi-permeable membrane for diffusion of oxygen, nutrients, and metabolic wastes between

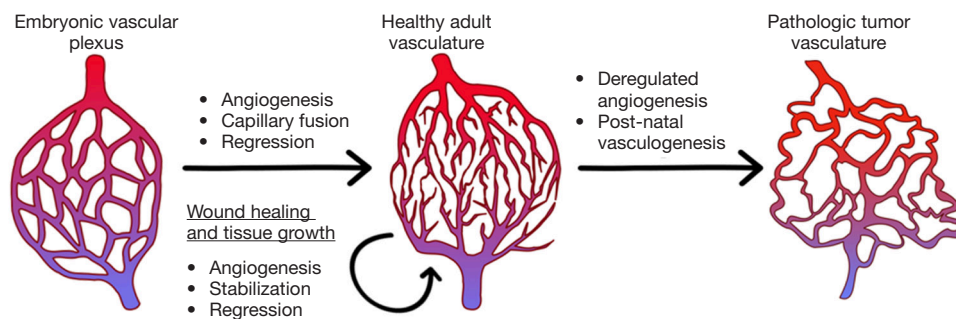


Figure 2 Development of hierarchical vascular structure from embryonic plexus (left panel) in healthy (central panel) and pathological tissues (right panel) [reproduced/adapted with permission from (7)].

the systemic circulation and local tissue environment, while the other inner layers are absent (11). Each type of cells performs a distinct function in maintenance of vascular homeostasis. The endothelium also influences the behaviour of SMCs, which are composed of several macromolecules such as collagen, lamellae and elastin.

Several attempts have been made in the last decade to mimic the vascular structure *in vitro*. Before the advent of microfluidics, the initial vascular models were mostly static platforms, which did not completely recapitulate the functions *in vivo* (12). Subsequently, vascular models were fabricated using technologies such as self-assembly, lithography patterning, use of sacrificial templates, and pre-patterned micro-channel fabrication vasculature *in vitro*.

Vascular cells seeded within hydrogels can reconstitute 3D networks representing a physiologically-mimetic method for device fabrication. Using such an approach, anatomic flow conditions have been replicated in fibrin gel. Such devices have led to revelation of significant roles of pro-angiogenic factors in interstitial flow. Self-assembly of pro-vascular cells have been employed to generate several tissue-specific microvasculature microenvironments (6).

In other attempts, Human Umbilical Vein Endothelial Cells (HUVECs) were seeded on patterns created by photolithography (13). This process provides 2D perfusable biochips with optimum flow control and high-throughput capabilities. These techniques have also been extended to fabricate multi-layered polydimethylsiloxane (PDMS) chips (14). Other microfluidic methods have relied upon use of temporary molds, needles or rods made of materials such as gelatin, which are removed prior to cell seeding (6). In addition, vascular models inside bulk collagen gel have been used to study angiogenic sprouting or tumor-expressed angiogenic factors. However, most of these methods are inadequate to obtain the complex torturous structure of

vascular system as well as not able to fabricate structures with multiple cell types.

Bioprinting

In vivo models provide the most physiologically-relevant environment for studying tissue development and function, while the advancement of 3D bioprinting technology offers an enhanced feasibility and precision to tissue construct fabrication *in vitro*. 3D bioprinting offers a reproducible and scalable fabrication along with precise 3D control compared to conventional tissue fabrication methods. This 3D tissue fabrication has been improved to maintain high cell viability and normal function through the constructs.

Classification of bioprinting processes

Bioprinting processes can be classified into extrusion-, droplet- and laser-based bioprinting. Moreover, bioprinting of 3D vasculature can be performed through either scaffold-based or scaffold-free approaches. In extrusion- and droplet-based bioprinting, methods of fabrication can be further sub-classified into indirect or direct bioprinting. Indirect bioprinting involves the bioprinting of a sacrificial structure that is subsequently removed leaving behind the lumen. Direct bioprinting methods involve active bioprinting of hollow constructs with cell-loaded or cell-compatible bioinks. This method requires quick gelation/crosslinking to maintain a stable construct. Classification based on mechanism of scaffold-based bioprinting is expounded in the following subsections.

Extrusion-based bioprinting (EBB)

EBB is a process for the most bioinks at higher viscosities where bioinks are dispensed continuously out of the nozzle

by a pneumatic or mechanical screw plunger (15,16). Pneumatic-based bioprinting is a simple and extensively used method to drive biomaterials/cells from a syringe and nozzle at a controllable volume flow rate by compressed air. The flow properties and viscosity of the solution are the key parameters of material deposition (17). Biomaterial/cell solutions are mechanically pushed by a linear moving piston or a screw driver in piston-based bioprinting (18), which provides large deposition force. In the dispensing process, EBB is compatible with a wide range of fluid viscosities. Higher viscosity materials are more suitable in terms of providing structural support for the tissue scaffolds while lower viscosity materials are more appropriate for cellular bioactivities (19,20). Increasing the diameter of dispensed filaments can increase the mechanical stability of structures, which however prevents the exchange of nutrients and metabolic wastes. On the other hand, reducing the diameter of filaments can eliminate diffusion barriers but weaken mechanical properties. Various crosslinking mechanism with respect to temperature, ionic bonding and covalent bonding, is crucial for various hydrogel in bioprinting. Compared to DBB, EBB can be applied to various materials such as viscous polymers and cell-encapsulated hydrogels at high cell density. The cell viability is significantly compromised with the increase of extrusion pressure due to the higher shear stress applied to cells.

Droplet-based bioprinting (DBB)

DBB is a non-contact technique, which was first introduced about 20 years ago. It reproduces digital pattern information onto a substrate with tiny ink droplets and generates constructs in a layer-by-layer approach. The bioinks used in DBB include hydrogels, living cells, and biological substances (21). The droplets for bioprinting can be generated by thermal, piezoelectric, or electromagnetic actuation mechanisms. However, in DBB, the range of viscosities of bioink is limited due to forces of actuation that can be attained. Moreover, high viscosity of the bioink and high cell density may lead to uneven deposition and nozzle clogging (8). The small print head orifices may also cause high shear force to the bioprinted cells which can cause damage to the cell membrane, leading to cell death (22-25).

Laser-based bioprinting (LBB)

LBB is based on the principles of laser-induced forward transfer or vat photopolymerization (8,26). Vat photopolymerization is a very fast and continuous 3D printing process. It is based on hardening of photopolymer on exposure to the ultraviolet

radiation. Stereolithography (SLA) is the traditional technique in which light patterning is accomplished by vector scanning, mask projection or two-photon polymerization techniques (27). Continuous liquid interface production (CLIP) has been developed as a new technique, which particularly accords fabrication of overhang structures (28). The major components of a laser bioprinter include a pulsed laser beam source, a focusing system, a target plate, and a collector substrate slide. A ribbon is also included to support the donor layer. The top layer of the ribbon is usually made of gold or titanium to absorb the energy of the laser beam and the bottom layer is loaded with a bioink. During the bioprinting process, a laser pulse is focused onto the top layer. The absorbed energy produces a bubble in the bottom layer and the generated shock waves push the bioink out of the ribbon into the collector slide. The bioprinting resolution of LBB depends on laser energy, pulse frequency, layer thickness and bioink viscosity, the distance between donor and collector layers as well as the substrate wettability. LBB is the only nozzle- and orifice-free printing technology. The problem of nozzle clogging does not exist in LBB. Since there are no nozzles, the bioink viscosities can vary from 1 to 300 mPa·s. Higher bioprinting resolution is another advantage of LBB (29-32). The drawbacks of LBB processes can be discussed in two groups. Laser-induced forward transfer is a tedious and time consuming process with a high cost of instrumentation. A complex set of process parameters are involved with nonlinear physical interactions. In addition, this process requires a metal film and thus is subject to metallic particle contamination. Vat polymerization processes, on the other hand, are compatible with a limited number of bioinks, which is further constrained with other issues such as the toxicity concerns of UV light and photoinitiators (33).

Early studies on acellular printing of vasculature

Several studies for bioprinting of vasculature can be considered to be inspired by traditional 3D printing techniques for obtaining vascular models (34). The results of vascular models fabricated by 3D printing technologies (i.e., without use of cell as bioink components) provide useful appraisal on the channel dimensions required for bioprinting of vascular constructs. For example, Yang *et al.* have utilized 3D printing-enabled hydrogel casting for developing microfluidic vascular channels (35). The presented process in his work contained three major steps. Initially, murine 10T1/2 cells were UV crosslinked within gelatin methacrylate (GelMA) hydrogel. Following template

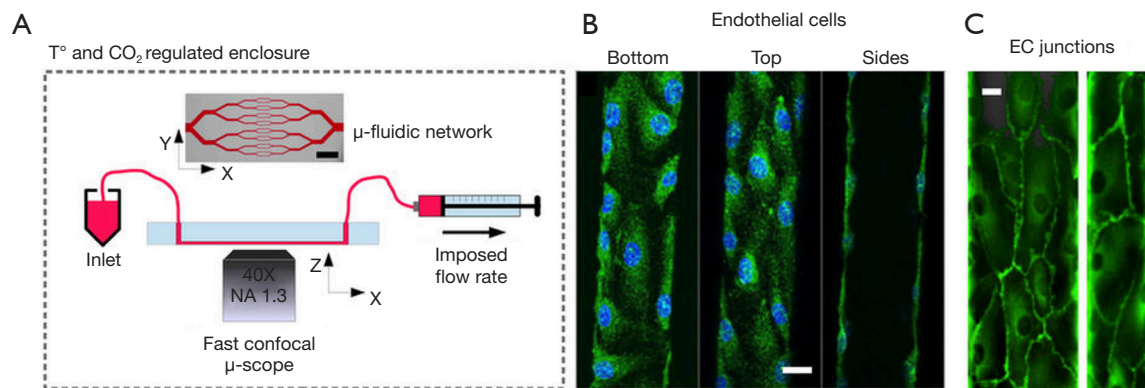


Figure 3 Branching architectures constantly perfused with culture medium and adherence of endothelial cells adhered the walls of a micro-channel [reproduced with permission from (38)].

casting, they developed a hollow L-shaped channel within GelMA with confluent endothelium lining and sufficient cell viability. Afterwards, HUVECs were cultured within the channel and visualization of endothelial monolayers was achieved through immunostaining. Furthermore, the barrier function of HUVEC monolayer was indicated by diffusion/permeability studies on endothelialized channels (35). Similarly, Zhang *et al.* have developed hydrogel chips, in which 3D microfluidic channel networks with physiologically-relevant size was embedded by SLA, to provide long-term perfusion (36). A layer of pre-polymer of PDMS was cast against photosensitive material coated silicon mold to construct similar topography from PDMS substrate. The microfluidic device was developed from this substrate by further bonding with blank PDMS slab or cover glass. An aqueous resin composed of poly (ethylene glycol diacrylate) (PEGDA), photoinitiator (lithiumphenyl-2,4,6-trimethylbenzoylphosphinate, LAP) and photoabsorber (quinoline yellow, QY) was developed for SLA-based printing. Although microchannels with cross-section as small as $200\ \mu\text{m} \times 200\ \mu\text{m}$ could be printed, perfusion of printed microchannels could only be achieved in channels with larger cross-section (at least $300\ \mu\text{m} \times 300\ \mu\text{m}$). Similarly, a hybrid 3D printing technique has also been demonstrated for vasculature-on-a-chip applications. This is reflected in work of Liu *et al.* who have fabricated a variable height micro-mixer (VHM) using projection 3D printing combined with soft lithography (37). Soft lithographic based fabrication of microchannels have also been demonstrated to form confluent endothelial cells layer the walls of the channels along with expression of a *in vivo*-mimetic 600 nm glycocalyx layer within the lumens, as shown Figure 3 (38).

In situ user-defined cell-laden scaffolds were directly printed in VHM. PDMS was used in micro-casting the PEGDA-based structural mold. This study described the ability of efficiently mixing two fluids within a microfluidic device such that a tissue scaffold can be printed *in situ* within the device. Microfluidic mixers with low flow rate can be used in a wide variety of applications where in-device mixing of reagents is preferable to pre-mixing external to the device. For example, mixing live cells with pre-polymer solutions may be deleterious. 3D printing using nano-hydroxyapatite as a material and biomimetic micro-channel architecture designed in CAD software has also resulted in the formation of vascularized bone tissue constructs (39).

Bioprinting for vasculature modelling

EBB has been the most widely employed technique for fabrication of vascular constructs using direct extrusion as well as indirect extrusion with the aid of fugitive inks. In direct extrusion methods, bioinks containing cells with hydrogels are directly extruded as per design. Post-extrusion, bioink components are solidified in a physiologically amenable environment to provide constructs with acceptable mechanically and biologically compatible properties. In EBB, cell viability is affected by method of solidification and shear-induced stresses experienced by cells. Examples of EBB for vascular tissue fabrication can be found in the work of Li *et al.*, who constructed vascularized liver tissue using a dual nozzle extrusion bioprinting with two cell-laden bioinks (i.e., gelatin/alginate/chitosan hydrogel containing hepatocytes and gelatin/alginate/fibrinogen containing adipose derived stem cells (ADSCs)

on a cooled substrate (40). The multiple compositions of hydrogels provided both immediate crosslinking due to presence of alginate and long-term cell viability due to presence of gelatin, fibrinogen, or chitosan. In this method, mixture of thrombin, calcium, and sodium triphosphate was used for crosslinking wherein proliferation and histochemical assays indicated appreciable cell survival. An affordable extrusion bioprinter, Fab@Home, was demonstrated to be capable of forming vessel-like constructs using polyethylene glycol (PEG) pentaerythritol derivatives co-crosslinked with gelatin and sulphated hyaluronic acid (41). Though bioprinted NIH 3T3 cells exhibited significant viability, formation of vascularized perfusable constructs using this system have not been reported so far. There have been similar efforts showing promise for fabricating constructs with hollow channels of different diameters. In most such cases, alginate has been the popular option, and hollow channels up to 15 mm in height has been successfully fabricated (42). To circumvent the stability concern on structural stability for fabricating constructs with large aspect ratio, some innovative approaches have been employed with the use of support baths. One of these techniques has been termed as freeform reversible embedding of suspended hydrogels (FRESH), which used support baths with Bingham plastic rheological behaviour, and hollow constructs with collagen, gelatin, myoblasts and fibroblasts have been fabricated into vascular network-like structures (43). Pinnock *et al.* have also presented an innovative method for producing customizable and self-organizing vascular constructs by replicating the tunica media (44). To form the vascular constructs, 3D printed inserts were first attached to tissue culture plates followed by the deposition of fibrin hydrogels around the inserts. It has the potential for future applications including disease modelling, drug testing, and studies of cell-cell interactions.

In bioprinting of vessel-like constructs, EBB has been modified to be dual-nozzle or coaxial extrusion processes. This concept was first introduced by Ozbolat and co-workers, in which different nozzle assemblies for feeding of hydrogel and crosslinker were used (45,46). The crosslinking was accomplished when hydrogel contacted the crosslinker solution at the tip of the coaxial nozzle. Bioprinting of human umbilical vein SMCs with alginate hydrogel using this process showed about 84% viability after seven days of perfusion culture (46,47). Based on coaxial extrusion, perfusable conduits up to sub-mm range in size were also demonstrated. For example, Novogen MMX Bioprinter™ have been used to fabricate constructs of 500–

1,500 µm outer diameter, 400–1,000 µm inner diameter, and 60–280 µm wall thickness using bioink composed of GelMA, multi-layered poly(ethylene glycol) acrylate derivate, sodium alginate and MSC and HUVEC as cell phase (48). Another variant of EBB has used microfluidic print head to substitute for coaxial head. This method has been shown to print GelMA with methacrylated hyaluronic acid (HAMA) and alginate bioinks, in which inner layers are solidified instantly while peripheral layers crosslink after some time lag due to diffusion of Ca^{2+} (48-51).

Bioprinting for perfusable constructs

In order to fabricate vascularized perfusable constructs, one of the most popular modifications of EBB is indirect bioprinting using fugitive inks. Fugitive inks or sacrificial inks are extruded in the form of solid tubular structures, followed by extrusion of other hydrogels as the bulk adjacent layers, and the initial sacrificial ink is then removed by dissolution leaving behind a hollow conduit in the gel. Through a two-step procedure, indirect EBB has been successfully explored for bioprinting of vascular models. Initial works in this direction were carried out using agarose as template bioink in constructs composed of several hydrogels including GelMA and poly(ethylene glycol) diacrylate (PEGDA) polymers (52). Perfusable microchannels lined with viable endothelial cell monolayers were successfully demonstrated. Human MSC-alginate-gelatin hydrogels were printed using dual-syringe layout with a thermal control, in which bioink at elevated temperatures was deposited onto a cooled (10 °C) substrate, and gelatin was used as a sacrificial bioink. This experiment also showed that bioprinting orientations can affect the cross-sectional area of bioprinted constructs (53). In one of most important works on fabricating perfusable constructs using fugitive works, Miller *et al.* employed a RepRap Mendel 3D printer using a glucose, sucrose and dextran mixture as a sacrificial phase (54). The sugar solution was first extruded at elevated temperatures, followed by manual injection of cells and hydrogels. Several hydrogels like PEGDA, fibrin-fibrinogen-thrombin and alginate were tested for feasibility along with several vascular architectures like curved filaments, perpendicular lattices, and Y-junctions of 150–750 µm in dimension. Important achievements of the work were the novel strategy for capillary formation and viable endothelial cells inside the perfusable channels with inner thickness up to 1 mm.

To overcome limitation of high temperature for removal

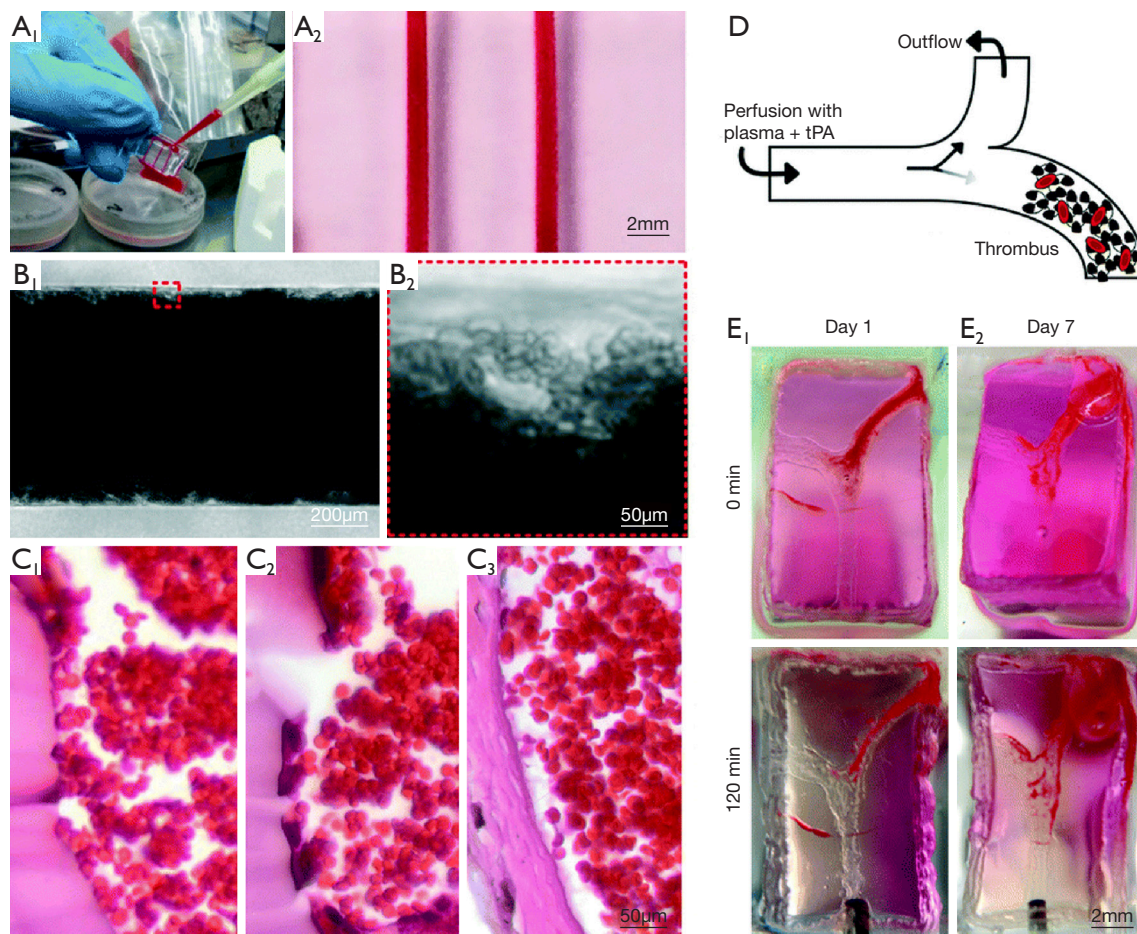


Figure 4 Thrombus formation and thrombolysis in a thrombosis-on-chip model shown by (A) perfusion of endothelial cells, (B) thrombus formed inside the channel, (C) H&E-stained sections of a thrombus with/without HUVECs on 7 days post-clotting, (D) schematic of thrombolytic study with tPA and (E) thrombolysis of clot on different time points [reproduced from (58) with permission of The Royal Society of Chemistry].

of sacrificial bioinks, perfusable microchannels have been built using Pluronic F127 as the sacrificial materials with PDMS, GelMA and human neonatal dermal fibroblast cells (HNFs)/10T1/2s/mouse fibroblast-laden bioink (55). Though fabrication of multi-layered constructs was accomplished, thick constructs could not be perfused directly and hence the bioprinted constructs were limited in long-term culture time (up to 14 days) or increased thickness (1–2 mm), which has prompted further research. Kolesky *et al.* fabricated a thick (e.g., over 1 cm) engineered bone tissue construct using fibrin/gelatin blended hydrogel and multiple cell types (56). Key idea of this scheme was to fabricate a perfusion chip and allow for generating viable constructs of over 1 cm thickness. The mold was fabricated using PDMS elastomer and a Pluronic F127/thrombin

blend fugitive ink. The cell-laden ink composed of gelatin, fibrinogen, transglutaminase and thrombin, was cast into the prefabricated mold and the fugitive ink was perfused out of the construct. Endothelial cells were then injected to perfuse the hollow tube for vascularization. Employing the same principles but using Pluronic as the sacrificial bioink, fabrication of an on-chip thrombosis model was achieved with fibroblasts and HUVECs embedded within GelMA. It has shown a perfused (up to 14 days) thrombosis-on-chip model using Pluronic as sacrificial bioink to form microchannels lined by HUVECs within a GelMA matrix loaded with fibroblasts (57,58). Both thrombus formation and thrombolysis has been recapitulated in this model as shown in *Figure 4*. In a similar study, EBB of Pluronic fugitive microvascular channels in a

collagen construct has been used to study evolution of microcirculatory architecture after angiogenesis. A better simulation of microenvironment of blood vessels in organ-on-a-chip devices can be achieved by multilevel fluidic channels in 3D hydrogel-based vascular structures fabricated using EBB. Endothelial cells can be seeded into the inner walls of a bioprinted tube template along with partially crosslinked hollow alginate filaments laden with fibroblasts and SMCs. The fusion of hollow filaments promoted development of two-level fluidic channels with a cylindrical macro-channel in the center and microchannels around the wall. The structures bioprinted using 4% alginate exhibited ultimate strength of 0.184 MPa, and the L929 mouse fibroblasts encapsulated in the constructs showed over 90% survival within one week. Moreover, bioprinting with three kinds of vascular cells exhibited uniform cell distribution with relatively high mechanical strength (5). Using agarose as a sacrificial material, micro-vessel-mimetic channels in the 3D liver constructs has been successfully printed using HepG2/C3A cells loaded GelMA as bulk hydrogel. HUVECs were seeded into the micro-channel for vascularization in the liver construct. Incorporation of vascular cells was found to delay permeation of molecules in the construct as well as an increase in survival of embedded cells in bulk constructs, and thus provided a physiologically-accurate vascularized model for drug screening (59).

Bioprinting vasculature with DBB

Several studies have demonstrated that DBB can be a suitable method to obtain vascularized structures. The first demonstration came with the use of a modified Hewlett-Packard (HP) bioprinter with hematopoietic stem cells-embedded hydrogel that was bioprinted in liquid media (60). The stem cells differentiated into multiple cell lineages after bioprinting. Further, Boland *et al.* obtained multi-layered cells-laden alginate constructs with uniform pore sizes, while the same group also fabricated micro-vessel constructs using Human Umbilical Vein Endothelial Cells (HUVECs)-laden bioink contained in pico-liter droplets with a thermal inkjet printer containing 50 firing nozzles (61). Rapid post-bioprinting gelation was achieved by using fibrinogen, thrombin and Ca^{2+} . Confluent HUVECs lining along branched tubular constructs resembling capillaries was observed after 21 days of culture. Electrostatic print head was applied to build alginate-based tubular constructs (with 35–40 μm thickness and 30–200 μm in inner diameter) in a CaCl_2 pool (62–64).

In DBB, piezoelectric print heads were also successfully used for vascular tissue bioprinting (65,66). Hemi-branching bifurcations and zigzag-shaped constructs composed of alginate and CaCl_2 has been well demonstrated (67). Interestingly, this work showed that buoyancy properties of CaCl_2 solution can be used to provide substantial support during bioprinting apart from acting as the crosslinking medium. DBB allowed both horizontal and vertical vessel-like bifurcations, maintaining with less than 10% cell damage (68). In another related approach, valve-based bioprinting of vascular conduits within a high-density fluorocarbon as liquid support bath was performed to obtain constructs with high aspect ratio of 30, without any significant loss of cell viability (96% to 99%) (69).

Similar to EBB, direct DBB is only suitable for creating *in vitro* models of blood vessels but not for fabrication of vascularized tissue models. For generating perfusable constructs, indirect DBB methods have found immense applicability. In indirect DBB with micro-valve bioprinters, gelatin has been used as a sacrificial bioink and was deposited in a cylindrical shape, which was successful to deposit cells (70). Gelatin was removed by temperature-induced decrosslinking. The conduits were then vascularized by endothelial cell seeding. To achieve this, a collagen layer in a flow chamber was first bioprinted. Thereafter, gelatin strands were bioprinted as a second layer followed by bioprinting of gelatin/HUVECs layer at room temperature for solidification of gelatin. Subsequently, a collagen layer was deposited as top layer and gelatin was liquefied by incubation at 37 °C leaving behind vascular channels in bulk hydrogel. Once the chamber was enclosed and physiological fluid flow conditions initiated, HUVECs proliferated and fully covered the inner surface within 2 to 3 days of dynamic culture compared to 70–80% of inner surface area coverage of the fluidic channel on Day 0. Immunostaining of E-cadherin showed that the confluent HUVEC monolayers formed adherent junctions on Day 5. The fluidic vascular channel was capable of supporting viability of tissue up to 5 mm in distance with 5 million cells/mL density under the physiological perfusion conditions. The same group has also shown fabrication of larger perfusable (lumen size of 1 mm) fluidic vascular channels wherein the spouting was initiated on Days 3–4 throughout the channel edge and extended up to 400 μm on Day 7 (71). The formation of capillary network and its integration within the construct is represented in *Figure 5*. Use of agarose as sacrificial template to bioprint hollow vessels within hydrogel constructs are also shown to be

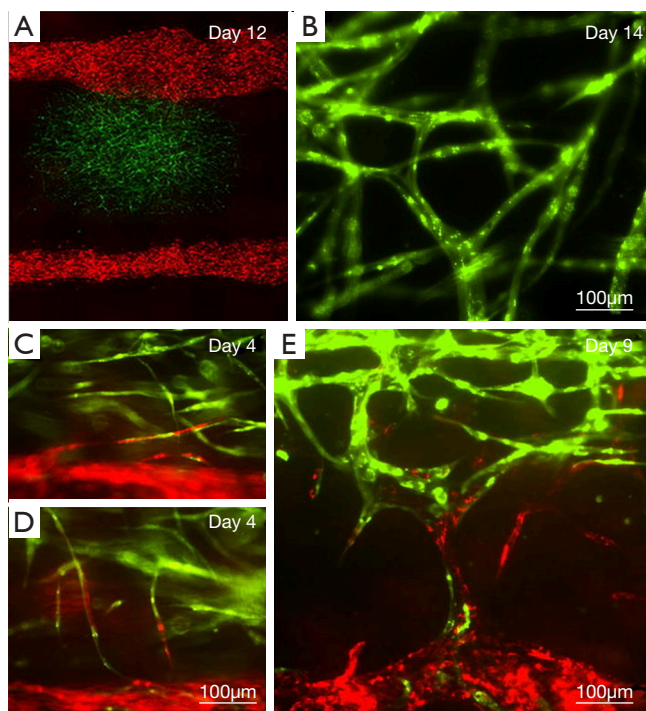


Figure 5 Two vascular channels and fibrin-cell mixture deposited in between. (A) HUVECs (green) were embedded within fibrin part for micro-vascularization. HUVECs (red) were seeded on the two fluidic channels to form vasculature. (B) HUVECs embedded within fibrin gel formed capillary network after 14 days of culture. (C,D,E) Integration of capillary network (green) and ECs sprouted from the parental vascular channel (red) [reprinted by permission from (71)].

possible with DBB, in which agarose solutions (>2 wt%) formed a solid gel below 32 °C to function as a fugitive bioink. A cell-laden hydrogel precursor [SMCs and fibroblasts in 5–20 wt% GelMA or polyethylene glycol diacrylate (PEGDA) solution] was then poured around the patterned agarose fibers and photo-crosslinked to form the matrix. Hollow channels with diameters down to 100 μm were achieved by removing agarose fibers under mild vacuum. Enhanced nutrient and oxygen delivery through these channels promoted the viability of surrounding stromal cells. Not only endothelium-coated microchannel but also smooth muscle, tunica intima and tunica adventitia can be assembled to recapitulate the biological function of the newly formed microvasculature. Due to an increase consumption of oxygen and nutrients caused by additional ECs embedded within the matrix around the channel, a considerable amount of cell death was observed.

LBB for vascular models

LBB has been used for branched vessel-like patterning of HUVECs, which evidently formed cell-cell interactions within a day post-bioprinting (72). The branched architectures exhibited very short stability. However, stability could be improved by bioprinting layer a human umbilical vein smooth muscle cells (HUVSMCs) above the HUVEC layer (72). Similarly, LBB can be used to form constructs made up of alginate hydrogel and mouse fibroblasts in the shape of stable 3D overhang bifurcated structures (73).

Digital light processing (DLP) based 3D printing is known for its superior speed, resolution, scalability and flexibility. A micr-oscale continuous optical bioprinting (mCOB) based on DLP can also be employed for developing pre-vascularized tissue at high speed and resolution (74). Bioprinting of endothelial cell and mesenchymal cells directly into designed vascular channels enabled perfusion and minimized the overall complexity and duration of the process. This process further promoted spontaneous *in vitro* formation of lumen-like structures of endothelial cells, and cell survival with progressive endothelial formation was also achieved in pre-vascularized tissue while implanted *in vivo*. Anastomosis between the bioprinted endothelial network and host circulation was observed with functional blood vessels containing red blood cells. Using various LBB platforms such as direct write (75) or biological laser printing (BioLPTM) (31,76,77) or laser induced forward transfer (LIFT) (78), several research groups independently fabricated cardiovascular models with endothelial cells, vascular smooth muscles, HUVECs and human MSCs with various combinations of alginate, polyester urethane urea (PEUU) and/or PEG acrylate hydrogels (78,79). Particularly with LIFT-based processes for cardiac patch bioprinting, improved vessel formation was evident. LBB has also shown successful pattern formation of vessel conduit on stackable collagen or porous poly-lactide-co-glycolide (PLGA) substrates (80). In an interesting advancement using near-infrared femtosecond laser, it has been observed that cell-laden collagen hydrogels can produce 3D vascular patterns *in situ* induced by absorption of laser energy by nano rods and resultant denaturation of adjacent collagen. The process can maintain high depositing speeds, and >90% cell viability with efficient migration of endothelial cells with 3D alignment thus presenting a facile technique for vascular tissue modelling (81). Digital micro-mirror device-based projection printing (DMD-PP) is another

LBB technique, which can be employed for fabrication of micro-channels with widths of 25–120 μm (82). Though above technique are suitable for fabricating vascular models, they have shown limited applicability for creating perfusable vascular channels for vascularized tissues modelling. However, a novel LBB technique, laser guided direct writing (LGDW) has been used by Nahmias *et al.* to form 2D and 3D patterns of HUVECs on MatrigelTM. Embedding HUVECs on MatrigelTM directed vasculature formation as per the design. Co-culturing of the vascular structure with hepatocytes resulted into formation of tubular structures which can be used for studying different biological processes involving heterotypic interactions such as liver and pancreas morphogenesis, or angiogenesis (83).

Scaffold-free vasculature bioprinting

Notwithstanding the pivotal role of scaffolding hydrogels in tissue engineering, hydrogels have also been considered to induce several inflammatory reactions, hindrance to tissue growth and non-approximation of native tissue mechanical properties due to differences with natural ECM. An alternative method to obtain vascular models by bioprinting is to use single cells or tissue spheroids as bioinks. Since last decade, it has been known that micro-tissues made of HUVEC-coated myofibroblasts can self-assemble to form macro-tissues with a simultaneously developed vascular system (84). Such vasculature could be easily integrated with the vascular system of a chicken embryo. Coaxial EBB has been demonstrated to fabricate tubular tissue strands with well-defined morphology by exploring the self-assembly of fibroblasts and insulinoma cells, which can be extended for vascular models. These tissue strands can be used for scale-up tissue biofabrication (85). The Multi-Arm BioPrinter is yet another platform for scale-up tissue bioprinting and can be integrated with a macro-level tubular vascular structure (45). Self-assembled fibroblast strands underwent fusion in a day and further tissue maturation was observed within a week, which yielded smooth muscle vascular constructs up to 1.5 cm in length. Histological examinations have further confirmed tight adhesion within the smooth muscle ECM, and the vasculature confirmed the potential for large-scale tissue models. Another pioneering achievement in this direction was demonstrated by the ability to fabricate multi-layered vascular models using HUVSMCs, porcine aortic smooth muscle cells (PASMCS) (86), and human skin fibroblasts (HSFs). In that study, cell pellet was extruded

into cylindrical shapes in capillary micropipettes capillary micropipettes (300–500 μm in diameters) and rounded off to smaller spheroids after culture. A mechanical ram-operated EBB system was used to dispense the spheroids inside an agarose mold to induce bifurcated shapes. In another study, tissue spheroids composed of endothelial cells and SMCs were bioprinted in to alginate molds, and fused to form vascular constructs with type-I collagen secreted by the proliferating cells. Bioprinting of pellet of mouse embryonic fibroblasts (MEF) with agarose support was also shown to mature to form aorta-like constructs (87). It is evident from scaffold-free bioprinting that a mold structure is still required to form large scale structures as cellular collagen deposition is usually very slow. Moreover, the mould can interact with bioprinted constructs and alter the biological, mechanical and chemical properties of the constructs. For example, due to strong bond between the support and construct, the removal of support material can result in mechanical damage to the tissue and break a part of the constructs. Moreover, cell aggregates (i.e., spheroids) often adhere to the support due to the deposition of ECM components at the boundary of cell aggregates and the mold. Cell aggregates (i.e., pellet) can also leak through the gaps at the interface of printed support structures. Continuous vascular channels within spheroid assembly accompanied by angiogenic sprouting and formation of anastomosis between two spheroids, were observed and can be used to form a contiguous vascular network. Self-assembly has also been exploited for bioprinting of a functional vascularized thyroid construct. It is embedded by using embryonic tissue spheroids and allantoic spheroids respectively in a collagen hydrogel. The embryonic tissue spheroids were observed to fuse into integrated constructs, along with formation of a capillary network around follicular cells, thus showing the promise of the approach to obtain vascularized tissue models (88). Several other cell types, which have shown promise towards formation of microvascular tissues, can also be explored for bioprinting vasculature. For example, culture of spheroidal micro-tissues that were made by embedding microvascular endothelial cells inside fibrin, exhibited the formation of endothelial sprouts (as shown in *Figure 6A*) (89). In a recent development, sprouting angiogenesis is demonstrated in islets engineered using mouse insulinoma endothelial cells under angiogenic conditions (see *Figure 6B*), which showed promise to be utilized for bioprinting of vascularized pancreatic models in the future (90).

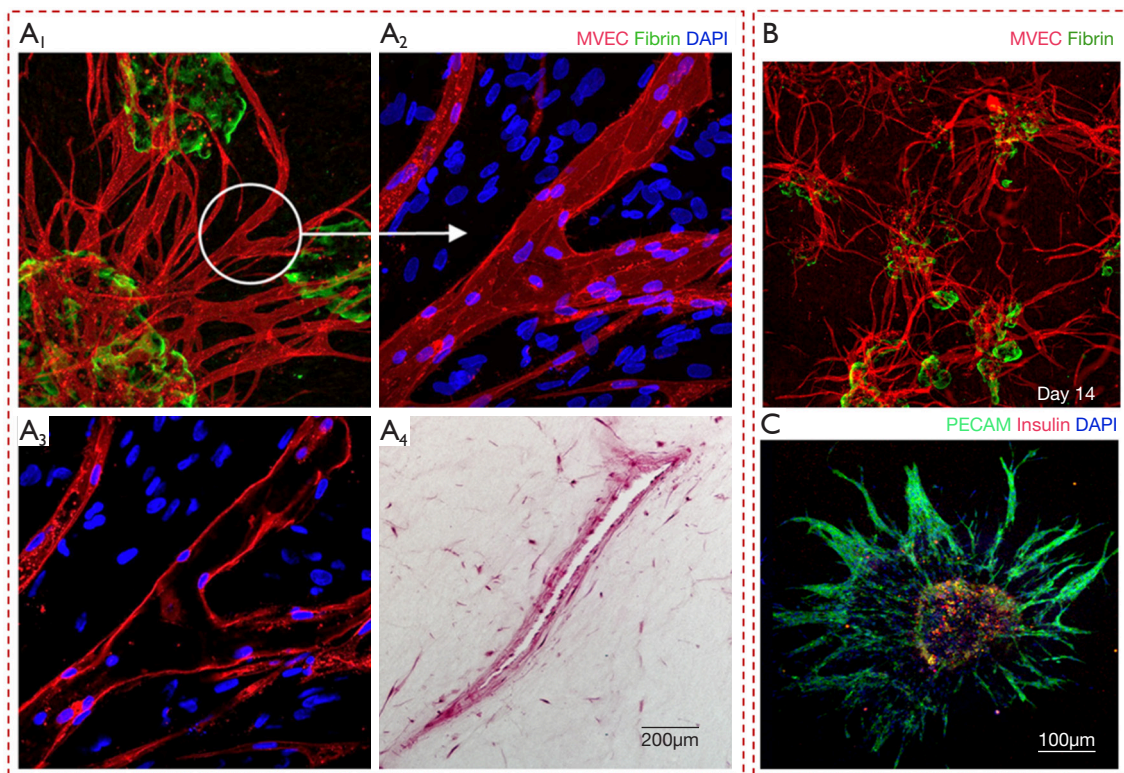


Figure 6 Bioprinting for formation of sprouting micro-vessels. (A) Formation of sprouting neovessels and (B) vessel networks inside micro-tissues embedded in fibrin hydrogel [reprinted (adapted) with permission from (89)]. (C) Immunocytochemistry images illustrating endothelial cells sprouting from pancreatic islets [reprinted (adapted) with permission from (90)].

Micro-vascular network models

Parallely, there have been efforts to fabricate micro-vasculature constructs like capillaries to overcome the practical limitations of bioprinting of large scale vascular networks. This is exemplified by bioprinting of vascularized bone constructs with various bioink components like Matrigel™, alginate, endothelial progenitor cells (EPCs) and multi-potent stromal cells. Bone tissue with notable vascularization was observed six weeks post bioprinting, though with inferior mechanical strength (91). Similarly, 3D cell-laden capillarized liver constructs were obtained after bioprinting hepatocytes, HUVECs, and human normal lung fibroblasts with collagen bioink over a polycaprolactone (PCL) frame using multi-head tissue/organ building system, as shown in Figure 6C (92). Encouraging results both with respect to hepatic tissue growth and capillary formation were evident. In another interesting work, 3D bioprinting with dual growth factors to pre-vascularized bone tissue has been attempted with human dental pulp stem cells

(DPSCs) as the cell source, which has both osteogenic and vasculogenic potential (93). The growth factors used for bioprinting were bone morphogenetic protein-2 (BMP-2) in the peripheral zone of the bioprinted construct, and the vascular endothelial growth factor (VEGF) in the central zone. DPSCs encapsulated within collagen type I with BMP-2, and gelatin/alginate mixed hydrogel with VEGF. It was seen that 60% of the encapsulated BMP-2 was released within seven days, and ~80% was consistently released by 40 days. Since pre-vascularized constructs showed promising results for *in vivo* bone regeneration purposes, such models can be ideal for studying bone growth *in vitro*.

Comparative evaluation of bioprinting technologies for vascular modelling

The principal consideration in selecting the correct bioprinting modality is based on the ability to generate constructs with adequate structural integrity, mechanical strength,

functionality of tissues, and anatomical accuracy. It is also logical to state that the choice of bioprinting modalities and bioinks would be influenced by the physiological considerations of the target tissue model wherein vascularization is desired. For example, EBB generally results in constructs with highest mechanical strength followed by DBB and LBB.

In general, EBB allows for fabrication of constructs with larger sizes or higher aspect ratios compared to DBB or LBB. While direct EBB is more suitable for bioprinting blood vessel models, indirect bioprinting has greater applicability for fabricating complex, porous and 3D vascularized models. In EBB, coaxial nozzle modality can be applied to generate constructs with higher aspect ratios; though obtaining branched structures still remains a challenge. The other great benefit of EBB is the indirect bioprinting approach, where fugitive inks can be easily bioprinted in highly complex patterns to generate open lumens for perfusion. However, stair stepping effects due to occlusions are observed during removal of sacrificial ink, which needs to be carefully considered before selecting the layer thickness with indirect EBB.

For vascularized bioprinting using indirect EBB, it has been observed that channels are easy to fabricate, but lining the lumen with endothelial cells or formation of tight junctions between the cells has still remained a challenge. Nevertheless, this appears to be a highly feasible technique for studying vasculature-related diseases or drug effects *in vitro*. While effects of drugs that are expected to act on endothelial cell receptors can be studied, many drugs are designed to act on receptors of vascular SMCs. For these studies, the concentric and multi-layered lumen should be fabricated inside the bulk hydrogel, which has been addressed till date. Moreover, when such multi-layered constructs (e.g., intimal, medial and adventitial layers) with heterogeneous material and cellular composition are fabricated, the different rate of growth of cellular components and different degradation rates of hydrogel components have to be taken into account. In absence of such designs, vascularized models might not be able to be stably perfused for the duration required for a particular biological investigation. Along with bioink selection, resolution of EBB would also require to be improved substantially to generate such heterogeneous constructs with high anatomical precision, which is probably the reason for the lack of micro-capillaries fabricated with EBB compared to DBB.

EBB is also utilized for fabrication of complex neurovascular

units (NVU). To maintain the brain health, the neural, vascular and ECM components form an inter-connected functional unit (94). Collagen with its slow gelation properties has been used to create mixed hydrogel-based bioinks with agarose, GelMA, MatrigelTM or alginate with altered shear thinning properties to create effective bioinks for bioprinting of neural and vascular cells. The combination of fibrin, hyaluronan and laminin was also used with neural and vascular stem cells to produce a 3D construct niche. This hydrogel took advantage of fibrin for neural stem cells, and crosslinked through interpenetrating networks of hyaluronan to mimic the native neural ECM (95). Also, two-photon lithography-based techniques will also be actively pursued for the purpose (94).

On the other hand, DBB provides superior bioprinting resolution, which is necessary to generate models of micro-capillaries. DBB also offers unique capabilities to bioprint co-culture models in pre-defined patterns with high-throughput, making them highly suitable for drug screening studies. The extremely small droplet sizes are probably the greatest advantage of DBB to fabricate the micro-vasculature models. However, the principal disadvantage of DBB is the inability to generate large scale vascular constructs. Therefore, DBB constructs may be considered more for investigations concerning micro-capillaries. Stand-alone constructs with low aspect ratio directly fabricated in a crosslinker bath has been demonstrated by DBB. Though their further mechanical characterization and bioprinting of supporting parenchyma tissue would be required before consideration for clinical transplantation, these models can be readily applied for *in vitro* biological testing, once evaluation under perfusion culture is performed. In DBB, indirect approach has already shown potential for oncological testing. Another limitation with DBB is the range of bioink viscosity that can be handled due to clogging issues. DBB also suffers from shear-stress that induces damage to cells, bioink sedimentation and cell-cell aggregation. As a consequence, bioinks are not all compatible with DBB, which reduces versatility of this technique.

The third bioprinting modality, LBB also presents unique advantages and disadvantages for fabrication of vasculature models. For example, LBB inspired by SLA has been used to generate branched configurations resembling native vasculature. However, cell densities compatible with EBB are less compared to both DBB and LBB. Like DBB, there exists constraint on the range of bioinks that can be processed as there are limited options of photo curable

hydrogels with photo-initiators, which is crucial for LBB. There are toxicity concerns of the photo curable hydrogels, photo initiators and the light (mostly UV), though effects of these agents are not all completely known. Since LBB constructs are mechanically inferior to EBB, the former may be considered more appropriate for fabricating tissue models than tissue engineering. The resolution of LBB is also higher than EBB. On the other hand, LBB causes reduced cell damage compared to both EBB and DBB and generally renders more than 95% cell viability. LBB bioprinters are also more sophisticated and expensive. Given the fact that hydrogel components of bioinks are major limitations for all bioprinting modalities, scaffold-free bioprinting of vascular models should be given more attention. One advantage of scaffold-free approach is that multi-cellular constructs are able to mature and deposit their own ECM (e.g., collagen and elastin) after cultivation in perfusion bioreactors. Several bioreactors can be designed to give additional mechanical stimulation to improve maturation rates. Such models can be more biomimetic and provide more physiologically-relevant information.

The relationship between cell density and mechanical properties of differently made constructs are the crucial factor in influencing the cellular viability and damage to cell membrane. During bioprinting of cells, mechanical strength i.e., shear stress has a negative impact on cellular viability, which leads to damage to cell membrane. So it is desirable to select low viscous (<10 mPa·s) bioinks with low cell densities (<10⁶ cells/mL) (96). The viscosity range of a bioink should be selected between 1 to 300 mPa·s for the LBB process (97). EBB Processes are able to print viscous bioinks (3×10⁷–6×10⁷ mPa·s) with a very high cell density without affecting cellular viability considerably (98). Less viscous bioinks (< 10 mPa·s) with lower cellular densities (<1.6×10⁶ cells/mL) is employed with inkjet bioprinting (99). Generally higher cell densities increase the viscosity of the bioink that results in clogging during bioprinting.

Conclusions and future perspectives

Developments in bioprinting are enabling the fabrication of vascular organ-on-a-chip models for more physiologically-accurate pathological and pharmacological investigations compared to conventional microfluidic devices. In this review, we have presented and analyzed the bioprinted vascular tissue constructs used for *in vitro* modelling of vessel functions. Applications of each of the bioprinting modalities along with their comparative assessment for

vasculature structure and function have been presented. Specific results of scaffold-free and scaffold-based bioprinting were also expounded with relation to their applicability for obtaining *in vitro* vascular models. However, achieving higher accuracies of material and architectural integrities is still required. Solving this problem would require future integration of different bioprinting modalities, bioinks and perfusion systems to allow long-term cultures. It would be also assumed significant to enhance bioprinting resolutions and culture condition with different biophysical stimulation to closer mimic *in vivo* behaviour. Another area of improvement would be the incorporation of different electrochemical and optical sensors for real-time and *in situ* monitoring of growth activities. The efforts would be in direction of obtaining functional organ-on-a-chip devices, which will be completely automated and consume less reagents and power. It is also observed that successful creation of such models will invariably need inputs from different disciplines including biological, material and instrumentation sciences. To date, bioprinted vascular models have revealed their potential, which can serve as an additional instrument for early disease and drug screening. The effect of ECM parameters can also be investigated within the bioprinted organ-on-chip constructs. Simultaneously, anatomy of native tissue should be understood in greater depths along with *in vivo/vitro* validations of the models. In following this manner, it may be expected that bioprinting can yield not only vascular models for drug testing but also for fabrication of vascular and vascularized organs.

Acknowledgments

Funding: This work has been supported by National Science Foundation Awards #1624515 and National Institutes of Health Award #1R21CA224422-01A1. The authors also acknowledge Department of Science and Technology, Government of India, INSPIRE Faculty Award to P Datta.

Footnote

Conflicts of Interest: All authors have completed the ICMJE uniform disclosure form (available at <http://dx.doi.org/10.21037/mps.2018.10.02>). The authors have no conflicts of interest to declare.

Ethical Statement: The authors are accountable for all aspects of the work in ensuring that questions related

to the accuracy or integrity of any part of the work are appropriately investigated and resolved.

Open Access Statement: This is an Open Access article distributed in accordance with the Creative Commons Attribution-NonCommercial-NoDerivs 4.0 International License (CC BY-NC-ND 4.0), which permits the non-commercial replication and distribution of the article with the strict proviso that no changes or edits are made and the original work is properly cited (including links to both the formal publication through the relevant DOI and the license). See: <https://creativecommons.org/licenses/by-nc-nd/4.0/>.

References

- Ghebre YT, Yakubov E, Wong WT, et al. Vascular Aging: Implications for Cardiovascular Disease and Therapy. *Transl Med (Sunnyvale)* 2016;6(4).
- Gorelick PB, Counts SE, Nyenhuis D. Vascular cognitive impairment and dementia. *Biochim Biophys Acta - Mol Basis Dis* 2016;1862:860-8.
- Fernandez CE, Yen RW, Perez SM, et al. Human Vascular Microphysiological System for in vitro Drug Screening. *Sci Rep* 2016;6:21579.
- Kimlin L, Kassir J, Virador V. 3D in vitro tissue models and their potential for drug screening. *Expert Opin Drug Discov* 2013;8:1455-66.
- Gao Q, Liu Z, Lin Z, et al. 3D Bioprinting of Vessel-like Structures with Multilevel Fluidic Channels. *ACS Biomater Sci Eng* 2017;3:399-408.
- Kim S, Kim W, Lim S, et al. Vasculature-On-A-Chip for In Vitro Disease Models. *Bioeng (Basel)* 2017;4(1).
- Paulsen SJ, Miller JS. Tissue vascularization through 3D printing: Will technology bring us flow? *Dev Dyn* 2015;244:629-40.
- Datta P, Ayan B, Ozbolat IT. Bioprinting for Vascular and Vascularized Tissue Biofabrication. *Acta Biomater* 2017;51:1-20.
- Berillis P. The Role of Collagen in the Aorta's Structure. *Open Circ Vasc J* 2013;6:1-8.
- Stegemann JP, Kaszuba SN, Rowe SL. Review: Advances in Vascular Tissue Engineering Using Protein-Based Biomaterials. *Tissue Eng* 2007;13:2601-13.
- Ardalani H, Assadi AH, Murphy WL. Structure, Function, and Development of Blood Vessels: Lessons for Tissue Engineering. In: Cai W. editor. *Engineering in Translational Medicine*. London: Springer London, 2014:155-82.
- Wong KHK, Chan JM, Kamm RD, et al. Microfluidic Models of Vascular Functions. *Annu Rev Biomed Eng* 2012;14:205-30.
- Gauvin R, Chen YC, Lee JW, et al. Microfabrication of complex porous tissue engineering scaffolds using 3D projection stereolithography. *Biomaterials* 2012;33:3824-34.
- Xu Z, Li E, Guo Z, et al. Design and Construction of a Multi-Organ Microfluidic Chip Mimicking the in vivo Microenvironment of Lung Cancer Metastasis. *ACS Appl Mater Interfaces* 2016;8:25840-7.
- Ozbolat IT, Hospodiuk M. Current advances and future perspectives in extrusion-based bioprinting. *Biomaterials* 2016;76:321-43.
- Hospodiuk M, Moncal KK, Dey M, et al. Extrusion-Based Biofabrication in Tissue Engineering and Regenerative Medicine. In: Ovsianikov A, Yoo J, Mironov V. editors. *3D Printing and Biofabrication*. Cham: Springer International Publishing, 2016:1-27.
- Ning L, Chen X. A brief review of extrusion-based tissue scaffold bio-printing. *Biotechnol J* 2017;12(8).
- Valkenaers H, Vogeler F, Voet A, et al. Screw extrusion based 3D printing, a novel additive manufacturing technology. *Coma'13* 2013.
- Little CJ, Bawolin NK, Chen X. Mechanical Properties of Natural Cartilage and Tissue-Engineered Constructs. *Tissue Eng Part B Rev* 2011;17:213-27.
- Bian L, Hou C, Tous E, et al. The influence of hyaluronic acid hydrogel crosslinking density and macromolecular diffusivity on human MSC chondrogenesis and hypertrophy. *Biomaterials* 2013;34:413-21.
- Gudapati H, Dey M, Ozbolat I. A comprehensive review on droplet-based bioprinting: Past, present and future. *Biomaterials* 2016;102:20-42.
- Cui X, Boland T, D'Lima DD, et al. Thermal Inkjet Printing in Tissue Engineering and Regenerative Medicine. *Recent Patents Drug Deliv Formul* 2012;6:149-55.
- Ozbolat IT, Moncal KK, Gudapati H, et al. Evaluation of bioprinter technologies. *Addit Manuf* 2017;13:179-200.
- Zohora FT, Yousuf A, Anwarul M, et al. Inkjet printing : an emerging technology for 3d tissue or organ printing. *Eur Sci J* 2014;10:339-52.
- Ozbolat IT, Yu Y. Bioprinting Toward Organ Fabrication : Challenges and Future Trends. *IEEE Trans Biomed Eng* 2013;60:691-9.
- Shashi GM, Laskar MAR, Biswas H, et al. A Brief Review of Additive Manufacturing with Applications. *Proc 14th*

- Glob Eng Technol Conf 2017.
27. Chartrain NA, Williams CB, Whittington AR. A Review on Fabricating Tissue Scaffolds using Vat Photopolymerization. *Acta Biomater* 2018;74:90-111.
 28. Januszewicz R, Tumbleston JR, Quintanilla AL, et al. Layerless fabrication with continuous liquid interface production. *Proc Natl Acad Sci* 2016;113:11703-8.
 29. Gruene M, Unger C, Koch L, et al. Dispensing pico to nanolitre of a natural hydrogel by laser-assisted bioprinting. *Biomed Eng Online* 2011;10:19.
 30. Gruene M, Deiwick A, Koch L, et al. Laser Printing of Stem Cells for Biofabrication of Scaffold-Free Autologous Grafts. *Tissue Eng Part C Methods* 2011;17:79-87.
 31. Koch L, Gruene M, Unger C, et al. Laser assisted cell printing. *Curr Pharm Biotechnol* 2013;14:91-7.
 32. Ringeisen BR, Barron JA, Young D, et al. Laser Printing Cells BT - Virtual Prototyping & Bio Manufacturing in Medical Applications. In: Bidanda B, Bártolo P. editors. Boston, MA: Springer US, 2008:207-28.
 33. Datta P, Barui A, Wu Y, et al. Essential steps in bioprinting: From pre- to post-bioprinting. *Biotechnol Adv* 2018;36:1481-504.
 34. Mafeld S, Nesbitt C, McCaslin J, et al. Three-dimensional (3D) printed endovascular simulation models: a feasibility study. *Ann Transl Med* 2017;5:42.
 35. Yang L, Shridhar SV, Gerwitz M, et al. An in vitro vascular chip using 3D printing-enabled hydrogel casting. *Biofabrication* 2016;8:035015.
 36. Zhang R, Larsen NB. Stereolithographic hydrogel printing of 3D culture chips with biofunctionalized complex 3D perfusion networks. *Lab Chip* 2017;17:4273-82.
 37. Liu J, Hwang HH, Wang P, et al. Direct 3D-printing of cell-laden constructs in microfluidic architectures. *Lab Chip* 2016;16:1430-8.
 38. Tsvirkun D, Grichine A, Duperray A, et al. Microvasculature on a chip: study of the Endothelial Surface Layer and the flow structure of Red Blood Cells. *Sci Rep* 2017;7:45036.
 39. Holmes B, Bulusu K, Plesniak M, et al. A synergistic approach to the design, fabrication and evaluation of 3D printed micro and nano featured scaffolds for vascularized bone tissue repair. *Nanotechnology* 2016;27:064001.
 40. Shengjie L, Xiong Z, Wang X, et al. Direct fabrication of a hybrid cell/hydrogel construct by a double-nozzle assembling technology. *J Bioact Compat Polym* 2009;24:249-65.
 41. Skardal A, Zhang J, Mccoard L, et al. Photocrosslinkable Hyaluronan-Gelatin Hydrogels for Two-Step Bioprinting. *Tissue Eng Part A* 2010;16:2675-85.
 42. Tan EYS, Yeong WY. Concentric bioprinting of alginate-based tubular constructs using multi-nozzle extrusion-based technique. *Int J Bioprinting* 2015;1:49-56.
 43. Hinton TJ, Jallerat Q, Palchesko RN, et al. Three-dimensional printing of complex biological structures by freeform reversible embedding of suspended hydrogels. *Sci Adv* 2015;1:e1500758.
 44. Pinnock CB, Meier EM, Joshi NN, et al. Customizable engineered blood vessels using 3D printed inserts. *Methods* 2016;99:20-7.
 45. Ozbolat IT, Chen H, Yu Y. Development of “Multi-arm Bioprinter” for hybrid biofabrication of tissue engineering constructs. *Robot Comput Integr Manuf* 2014;30:295-304.
 46. Zhang Y, Yu Y, Akkouch A, et al. In vitro study of directly bioprinted perfusable vasculature conduits. *Biomater Sci* 2015;3:134-43.
 47. Zhang Y, Yu Y, Chen H, et al. Characterization of Printable Cellular Micro-fluidic Channels for Tissue Engineering. *Biofabrication* 2013;5:025004.
 48. Jia W, Gungor-Ozkerim PS, Zhang YS. Direct 3D bioprinting of perfusable vascular constructs using a blend bioink. *Biomaterials* 2016;106:58-68.
 49. Attalla R, Selvaganapathy PR. 3D printing of gels with integrated vascular channels for cell culture using a microfluidic printhead. In: 18th International Conference on Miniaturized Systems for Chemistry and Life Sciences. San Antonio, Texas, USA, 2014:479-81.
 50. Attalla R, Ling C, Selvaganapathy P, et al. Fabrication and characterization of gels with integrated channels using 3D printing with microfluidic nozzle for tissue engineering applications. *Biomed Microdevices* 2016;18:17.
 51. Selvaganapathy PR, Attala R. Microfluidic vascular channels in gels using commercial 3D printers. In: Gray; BL, Becker H, editors. *Proc SPIE 9705, Microfluidics, BioMEMS, and Medical Microsystems XIV*, 97050J. San Francisco, California, United States, 2016:3-4.
 52. Bertassoni LE, Cecconi M, Manoharan V, et al. Hydrogel bioprinted microchannel networks for vascularization of tissue engineering constructs. *Lab Chip* 2014;14:2202-11.
 53. Wüst S, Muller R, Hoffman S. 3D Bioprinting of complex channels — Effects of material, orientation, geometry, and cell embedding. *J Biomed Mater Res A* 2015;103:2558-70.
 54. Miller JS, Stevens KR, Yang MT, et al. Rapid casting of patterned vascular networks for perfusable engineered three-dimensional tissues. *Nat Mater* 2012;11:768-74.
 55. Kolesky DB, Truby RL, Gladman AS, et al. 3D bioprinting of vascularized, heterogeneous cell-laden tissue constructs.

- Adv Mater 2014;26:3124-30.
56. Kolesky DB, Homan KA, Skylar-Scott MA, et al. Three-dimensional bioprinting of thick vascularized tissues. *Proc Natl Acad Sci* 2016;113:3179-84.
 57. Oklu R, Zhang Y, Albadawi H, et al. 3D bioprinted thrombosis-on-a-chip model. *J Vasc Interv Radiol* 2017;28:S146.
 58. Zhang YS, Davoudi F, Walch P, et al. Bioprinted thrombosis-on-a-chip. *Lab Chip* 2016;16:4097-105.
 59. Massa S, Sakr MA, Seo J, et al. Bioprinted 3D vascularized tissue model for drug toxicity analysis. *Biomicrofluidics* 2017;11:044109.
 60. Kesari P, Xu T, Boland T. Layer-by-layer printing of cells and its application to tissue engineering. *MRS Online Proc Libr Arch* 2004;845:AA4.5.
 61. Boland T, Tao X, Damon BJ, et al. Drop-on-demand printing of cells and materials for designer tissue constructs. *Mater Sci Eng C* 2007;27:372-6.
 62. Arai K, Iwanaga S, Toda H, et al. Three-dimensional inkjet biofabrication based on designed images. *Biofabrication* 2011;3:034113.
 63. Nakamura M, Kobayashi A, Takagi F, et al. Biocompatible inkjet printing technique for designed seeding of individual living cells. *Tissue Eng* 2005;11:1658-66.
 64. Nakamura M, Nishiyama Y, Henmi C, et al. Ink jet three-dimensional digital fabrication for biological tissue manufacturing: analysis of alginate microgel beads produced by ink jet droplets for three dimensional tissue fabrication. *J Imaging Sci Technol* 2008;52:60201-1-60201-6.
 65. Xu C, Zhang Z, Christensen K, et al. Freeform Vertical and Horizontal Fabrication of Alginate-Based Vascular-Like Tubular Constructs Using Inkjetting. *J Manuf Sci Eng* 2014;136:061020.
 66. Xu C, Zhang M, Huang Y, et al. Study of Droplet Formation Process during Drop-on-Demand Inkjetting of Living Cell-Laden Bioink. *Langmuir* 2014;30:9130-8.
 67. Xu C, Chai W, Huang Y, et al. Scaffold-free inkjet printing of threedimensional zigzag cellular tubes. *Biotechnol Bioeng* 2012;109:3152-60.
 68. Christensen K, Xu C, Chai W, et al. Freeform inkjet printing of cellular structures with bifurcations. *Biotechnol Bioeng* 2015;112:1047-55.
 69. Duarte Campos DF, Blaeser A, Weber M, et al. Three-dimensional printing of stem cell-laden hydrogels submerged in a hydrophobic high-density fluid. *Biofabrication* 2013;5:015003.
 70. Lee VK, Kim DY, Ngo H, et al. Creating perfused functional vascular channels using 3D bio-printing technology. *Biomaterials* 2014;35:8092-102.
 71. Lee VK, Lanzi AM, Haygan N, et al. Generation of Multi-Scale Vascular Network System within 3D Hydrogel using 3D Bio-Printing Technology. *Cell Mol Bioeng* 2014;7:460-72.
 72. Wu PK, Ringeisen BR. Development of human umbilical vein endothelial cell (HUVEC) and human umbilical vein smooth muscle cell (HUVSMC) branch/stem structures on hydrogel layers via biological laser printing (BioLP). *Biofabrication* 2010;2:014111.
 73. Xiong R, Zhang Z, Chai W, et al. Freeform drop-on-demand laser printing of 3D alginate and cellular constructs. *Biofabrication* 2015;7:045011.
 74. Zhu W, Qu X, Zhu J, et al. Direct 3D bioprinting of prevascularized tissue constructs with complex microarchitecture. *Biomaterials* 2017;124:106-15.
 75. Hribar KC, Soman P, Warner J, et al. Light-assisted direct-write of 3D functional biomaterials. *Lab Chip* 2014;14:268-75.
 76. Barron JA, Wu P, Ladouceur HD, et al. Biological laser printing: a novel technique for creating heterogeneous 3-dimensional cell patterns. *Biomed Microdevices* 2004;6:139-47.
 77. Ovsianikov A, Gruene M, Pflaum M, et al. Laser printing of cells into 3D scaffolds. *Biofabrication* 2010;2:014104.
 78. Gaebel R, Ma N, Liu J, et al. Patterning human stem cells and endothelial cells with laser printing for cardiac regeneration. *Biomaterials* 2011;32:9218-30.
 79. Devillard R, Pagès E, Correa MM, et al. Chapter 9 - Cell Patterning by Laser-Assisted Bioprinting. *Methods in Cell Biology* 2014;119:159-74.
 80. Pirlo RK, Wu P, Liu J, et al. PLGA/hydrogel biopapers as a stackable substrate for printing HUVEC networks via BioLPTM. *Biotechnol Bioeng* 2012;109:262-73.
 81. Hribar KC, Meggs K, Liu J, et al. Three-dimensional direct cell patterning in collagen hydrogels with near-infrared femtosecond laser. *Sci Rep* 2015;5:17203.
 82. Huang TQ, Qu X, Liu J, et al. 3D printing of biomimetic microstructures for cancer cell migration. *Biomed Microdevices* 2014;16:127-32.
 83. Nahmias Y, Schwartz RE, Verfaillie CM, et al. Laser-guided direct writing for three-dimensional tissue engineering. *Biotechnol Bioeng* 2005;92:129-36.
 84. Kelm JM, Djonov V, Ittne LM, et al. Design of Custom-Shaped Vascularized Tissues Using Microtissue Spheroids as Minimal Building Units. *Tissue Eng* 2006;12:2151-60.
 85. Akkouch A, Yu Y, Ozbolat IT. Microfabrication of

- scaffold-free tissue strands for three-dimensional tissue engineering. *Biofabrication* 2015;7:031002.
86. Norotte C, Marga FS, Niklason LE, et al. Scaffold-free vascular tissue engineering using bioprinting. *Biomaterials* 2009;30:5910-7.
 87. Kucukgul C, Ozler SB, Inci I, et al. 3D bioprinting of biomimetic aortic vascular constructs with self supporting cells. *Biotechnol Bioeng* 2015;112:811-21.
 88. Bulanova EA, Koudan EV, Degosserie J, et al. Bioprinting of a functional vascularized mouse thyroid gland construct. *Biofabrication* 2017;9:034105.
 89. Tiruvannamalai Annamalai R, Rioja AY, Putnam AJ, et al. Vascular Network Formation by Human Microvascular Endothelial Cells in Modular Fibrin Microtissues. *ACS Biomater Sci Eng* 2016;2:1914-25.
 90. Hospodiuk M, Dey M, Ayan B, et al. Sprouting angiogenesis in engineered pseudo islets. *Biofabrication* 2018;10:035003.
 91. Fedorovich NE, Oudshoorn MH, van Geemen D, et al. The effect of photopolymerization on stem cells embedded in hydrogels. *Biomaterials* 2009;30:344-53.
 92. Lee JW, Choi Y, Yong W, et al. Development of a 3D cell printed construct considering angiogenesis for liver tissue engineering. *Biofabrication* 2016;8:015007.
 93. Park JY, Shim JH, Choi SA, et al. 3D printing technology to control BMP-2 and VEGF delivery spatially and temporally to promote large-volume bone regeneration. *J Mater Chem B* 2015;3:5415-25.
 94. Han HW, Hsu S. Using 3D bioprinting to produce mini-brain. *Neural Regen Res* 2017;12:1595-6.
 95. Potjewyd G, Moxon S, Wang T, et al. Tissue Engineering 3D Neurovascular Units: A Biomaterials and Bioprinting Perspective. *Trends Biotechnol* 2018;36:457-72.
 96. Kim JD, Choi JS, Kim BS, et al. Piezoelectric inkjet printing of polymers: Stem cell patterning on polymer substrates. *Polymer (Guildf)* 2010;51:2147-54.
 97. Guillotin B, Souquet A, Catros S, et al. Laser assisted bioprinting of engineered tissue with high cell density and microscale organization. *Biomaterials* 2010;31:7250-6.
 98. Rasti H, Parivar K, Baharara J, et al. Chitin from the mollusc chiton: Extraction, characterization and chitosan preparation. *Iran J Pharm Res* 2017;16:366-79.
 99. Phillippi JA, Miller E, Weiss L, et al. Microenvironments Engineered by Inkjet Bioprinting Spatially Direct Adult Stem Cells Toward Muscle- and Bone-Like Subpopulations. *Stem Cells* 2008;26:127-34.

doi: 10.21037/mps.2018.10.02

Cite this article as: Sasmal P, Datta P, Wu Y, Ozbolat IT. 3D bioprinting for modelling vasculature. *Microphysiol Syst* 2018;2:9.